

1 **SEARCH FOR CORRELATIONS OF THE ARRIVAL**
2 **DIRECTIONS OF ULTRA-HIGH ENERGY COSMIC RAY**
3 **WITH EXTRAGALACTIC OBJECTS AS OBSERVED BY THE**
4 **TELESCOPE ARRAY EXPERIMENT**

5 T. ABU-ZAYYAD¹, R. AIDA², M. ALLEN¹, R. ANDERSON¹, R. AZUMA³,
6 E. BARCIKOWSKI¹, J.W. BELZ¹, D.R. BERGMAN¹, S.A. BLAKE¹, R. CADY¹,
7 B.G. CHEON⁴, J. CHIBA⁵, M. CHIKAWA⁶, E.J. CHO⁴, W.R. CHO⁷, H. FUJII⁸,
8 T. FUJII⁹, T. FUKUDA³, M. FUKUSHIMA^{10,11}, W. HANLON¹, K. HAYASHI³,
9 Y. HAYASHI⁹, N. HAYASHIDA¹⁰, K. HIBINO¹², K. HIYAMA¹⁰, K. HONDA²,
10 T. IGUCHI³, D. IKEDA¹⁰, K. IKUTA², N. INOUE¹³, T. ISHII², R. ISHIMORI³, H. ITO¹⁴,
11 D. IVANOV^{1,15}, S. IWAMOTO², C.C.H. JUI¹, K. KADOTA¹⁶, F. KAKIMOTO³,
12 O. KALASHEV¹⁷, T. KANBE², K. KASAHARA¹⁸, H. KAWAI¹⁹, S. KAWAKAMI⁹,
13 S. KAWANA¹³, E. KIDO¹⁰, H.B. KIM⁴, H.K. KIM⁷, J.H. KIM¹, J.H. KIM⁴,
14 K. KITAMOTO⁶, S. KITAMURA³, Y. KITAMURA³, K. KOBAYASHI⁵,
15 Y. KOBAYASHI³, Y. KONDO¹⁰, K. KURAMOTO⁹, V. KUZMIN¹⁷, Y.J. KWON⁷,
16 J. LAN¹, S.I. LIM²¹, J.P. LUNDQUIST¹, S. MACHIDA³, K. MARTENS¹¹,
17 T. MATSUDA⁸, T. MATSUURA³, T. MATSUYAMA⁹, J.N. MATTHEWS¹,
18 M. MINAMINO⁹, K. MIYATA⁵, Y. MURANO³, I. MYERS¹, K. NAGASAWA¹³,
19 S. NAGATAKI¹⁴, T. NAKAMURA²², S.W. NAM²¹, T. NONAKA¹⁰, S. OGIO⁹,
20 M. OHNISHI¹⁰, H. OHOKA¹⁰, K. OKI¹⁰, D. OKU², T. OKUDA²³, M. ONO¹⁴,
21 A. OSHIMA⁹, S. OZAWA¹⁸, I.H. PARK²⁴, M.S. PSIRKOV²⁵, D.C. RODRIGUEZ¹,
22 S.Y. ROH²⁰, G. RUBTSOV¹⁷, D. RYU²⁰, H. SAGAWA¹⁰, N. SAKURAI⁹,
23 A.L. SAMPSON¹, L.M. SCOTT¹⁵, P.D. SHAH¹, F. SHIBATA², T. SHIBATA¹⁰,
24 H. SHIMODAIRA¹⁰, B.K. SHIN⁴, J.I. SHIN⁷, T. SHIRAHAMA¹³, J.D. SMITH¹,
25 P. SOKOLSKY¹, R.W. SPRINGER¹, B.T. STOKES¹, S.R. STRATTON^{1,15},
26 T. STROMAN¹, S. SUZUKI⁸, Y. TAKAHASHI¹⁰, M. TAKEDA¹⁰, A. TAKETA²⁶,

27 M. TAKITA¹⁰, Y. TAMEDA¹⁰, H. TANAKA⁹, K. TANAKA²⁷, M. TANAKA⁹,
28 S.B. THOMAS¹, G.B. THOMSON¹, P. TINYAKOV^{17,25}, I. TKACHEV¹⁷, H. TOKUNO³,
29 T. TOMIDA²⁸, S. TROITSKY¹⁷, Y. TSUNESADA³, K. TSUTSUMI³,
30 Y. TSUYUGUCHI², Y. UCHIHORI²⁹, S. UDO¹², H. UKAI², F. URBAN²⁵,
31 G. VASILOFF¹, Y. WADA¹³, T. WONG¹, Y. YAMAKAWA¹⁰, R. YAMANE⁹,
32 H. YAMAOKA⁸, K. YAMAZAKI⁹, J. YANG²¹, Y. YONEDA⁹, S. YOSHIDA¹⁹,
33 H. YOSHII³⁰, X. ZHOU⁶, R. ZOLLINGER¹, Z. ZUNDEL¹

34
35 ¹High Energy Astrophysics Institute and Department of Physics and Astronomy,
36 University of Utah, Salt Lake City, Utah, USA

37 ²University of Yamanashi, Interdisciplinary Graduate School of Medicine and Engineering,
38 Kofu, Yamanashi, Japan

39 ³Graduate School of Science and Engineering, Tokyo Institute of Technology, Meguro,
40 Tokyo, Japan

41 ⁴Department of Physics and The Research Institute of Natural Science, Hanyang
42 University, Seongdong-gu, Seoul, Korea

43 ⁵Department of Physics, Tokyo University of Science, Noda, Chiba, Japan

44 ⁶Department of Physics, Kinki University, Higashi Osaka, Osaka, Japan

45 ⁷Department of Physics, Yonsei University, Seodaemun-gu, Seoul, Korea

46 ⁸Institute of Particle and Nuclear Studies, KEK, Tsukuba, Ibaraki, Japan

47 ⁹Graduate School of Science, Osaka City University, Osaka, Osaka, Japan

48 ¹⁰Institute for Cosmic Ray Research, University of Tokyo, Kashiwa, Chiba, Japan

49 ¹¹Kavli Institute for the Physics and Mathematics of the Universe (WPI), Todai Institutes
50 for Advanced Study, the University of Tokyo, Kashiwa, Chiba, Japan

51 ¹²Faculty of Engineering, Kanagawa University, Yokohama, Kanagawa, Japan

52 ¹³The Graduate School of Science and Engineering, Saitama University, Saitama, Saitama,

Japan

¹⁴Astrophysical Big Bang Laboratory, RIKEN, Wako, Saitama, Japan

¹⁵Department of Physics and Astronomy, Rutgers University, Piscataway, USA

¹⁶Department of Physics, Tokyo City University, Setagaya-ku, Tokyo, Japan

¹⁷Institute for Nuclear Research of the Russian Academy of Sciences, Moscow, Russia

¹⁸Advanced Research Institute for Science and Engineering, Waseda University,
Shinjuku-ku, Tokyo, Japan

¹⁹Department of Physics, Chiba University, Chiba, Chiba, Japan

²⁰Department of Astronomy and Space Science, Chungnam National University,
Yuseong-gu, Daejeon, Korea

²¹Department of Physics and Institute for the Early Universe, Ewha Womans University,
Seodaaemun-gu, Seoul, Korea

²²Faculty of Science, Kochi University, Kochi, Kochi, Japan

²³Department of Physical Sciences, Ritsumeikan University, Kusatsu, Shiga, Japan

²⁴Sungkyunkwan University, Jang-an-gu, Suwon, Korea

²⁵Service de Physique Théorique, Université Libre de Bruxelles, Brussels, Belgium

²⁶Earthquake Research Institute, University of Tokyo, Bunkyo-ku, Tokyo, Japan

²⁷Department of Physics, Hiroshima City University, Hiroshima, Hiroshima, Japan

²⁸Advanced Science Institute, RIKEN, Wako, Saitama, Japan

²⁹National Institute of Radiological Science, Chiba, Chiba, Japan

³⁰Department of Physics, Ehime University, Matsuyama, Ehime, Japan

Received _____; accepted _____

To be submitted to ApJ

ABSTRACT

75

76

78

79

80

81

82

83

84

85

86

87

88

89

90

We search for correlations between positions of extragalactic objects and arrival directions of Ultra-High Energy Cosmic Rays (UHECRs) with primary energy $E \geq 40$ EeV as observed by the surface detector array of the Telescope Array (TA) experiment during the first 40 months of operation. We examined several public astronomical object catalogs, including the Veron-Cetty and Veron catalog of active galactic nuclei. We counted the number of TA events correlated with objects in each catalog as a function of three parameters: the maximum angular separation between a TA event and an object, the minimum energy of the events, and the maximum redshift of the objects. We determine combinations of these parameters which maximize the correlations, and calculate the chance probabilities of having the same levels of correlations from an isotropic distribution of UHECR arrival directions. No statistically significant correlations are found when penalties for scanning over the above parameters and for searching in several catalogs are taken into account.

91

Subject headings: Astroparticle physics, cosmic rays, acceleration of particles

1. INTRODUCTION

92

93 Clarifying the origin of Ultra-High Energy Cosmic Rays (UHECRs) is one of the most
 94 important unsolved problems in modern astrophysics (e.g. Kotera & Olinto 2011). It is
 95 generally thought that cosmic rays with energies greater than 10^{18} eV (1 EeV) are of
 96 extragalactic origin because the Galactic magnetic fields are not strong enough to confine
 97 them. Indeed, no apparent anisotropy in arrival directions of UHECRs along the Galactic
 98 plane has been found. On the other hand, a steepening in the energy spectrum of UHECRs
 99 at around 50 EeV is observed by the High Resolution Fly’s Eye (HiRes) experiment and
 100 the Telescope Array (TA) experiment (Abbasi et al. 2008b; Abu-Zayyad et al. 2012b),
 101 and also by the Pierre Auger Observatory in a similar energy region (Abraham et al.
 102 2008, 2010). This can be explained as a consequence of the cosmic ray energy losses due
 103 to interactions with the Cosmic Microwave Background (CMB), as predicted by (Greisen
 104 1966), and (Zatsepin & Kuz’min 1966).

105 In this case, we expect that most of the observed cosmic rays of the highest energies
 106 originate from sources within the GZK horizon (~ 100 Mpc), and a correlation between
 107 nearby objects and arrival directions of cosmic rays is expected. The UHECRs are deflected
 108 by the Galactic and extragalactic magnetic fields on their way to Earth. The deflection
 109 angles are determined by the particle charges, source distances, and strength of the magnetic
 110 fields. For example, in case of a proton arriving from a 100 Mpc distance through a random
 111 extragalactic magnetic field 1 nG and correlation length of ~ 1 Mpc, the expected deflection
 112 angle is $3 - 5^\circ$ for 100 EeV (and less than 15° for 40 EeV) using the existing magnetic field
 113 estimates (Han et al. 2006; Sun et al. 2008; Pshirkov et al. 2011; Kronberg 1994).

114 The TA experiment observes UHECRs in the northern hemisphere using a Surface
 115 Detector (SD) array (Abu-Zayyad et al. 2012c) of ~ 700 km² area located in Millard County,
 116 Utah, USA (39.3° N, 112.9° W). Three Fluorescence Detector (FD) stations (Tokuno et al.

117 2012; Matthews et al. 2007) surround the SD array (Kawai et al. 2008) and view the
118 atmosphere above it. The SD array consists of 507 SDs installed on a square grid with
119 1.2 km spacing, and measures particles from Extensive Air Showers (EASs) at ground level.
120 The energy and the arrival direction of a primary particle are determined from observed
121 energy deposits as a function of distance from the shower core in the SDs and the arrival
122 time distribution of the EAS particles. The test operation of the SD array began in March
123 2008, and the full SD array has been operational with a uniform trigger criteria from May
124 11, 2008. The present analysis uses only the events detected by the SD array because this
125 data set has the greatest statistics than that by the FDs.

126 Assuming the sources have the same intrinsic UHECR luminosities, the arrival
127 directions of higher energy cosmic rays from nearby sources are expected to correlate
128 better with the source positions. We search for the correlations between the TA events
129 and objects in catalogs by changing three parameters: the minimum energy of the cosmic
130 ray events, E_{\min} , the separation angle, ψ , between the cosmic ray arrival direction and
131 the object, and the maximum redshift, z_{\max} , of the objects. A similar approach has
132 been taken in the analyses by the Pierre Auger Observatory (Abreu et al. 2007, 2008,
133 2010) and by the HiRes experiment (Abbasi et al. 2008a) using the VCV catalog of 12th
134 edition (Veron-Cetty & Veron 2006).

135 As putative sources of UHECR, we examine the objects in the 13th edition of the
136 VCV catalog (Veron-Cetty & Veron 2010). This catalog is a compilation of several surveys
137 made under different conditions such as Field Of Views (FOVs), observation periods,
138 etc. It does not represent a homogeneous sample of Active Galactic Nuclei (AGNs),
139 and its degree of completeness is unknown (Veron-Cetty & Veron 2010). In addition,
140 we have investigated unbiased data sets from different measurements, namely, radio:
141 the third Cambridge catalog of radio sources catalog (3CRR) (Laing, Riley & Longair

142 1983), infrared: the 2MASS (the Two Micron All-Sky Survey) redshift survey catalog
143 (2MRS) (Huchra et al. 2012), X-Ray: Swift BAT (Burst Alert Telescope) 58-Month hard
144 X-ray survey catalog (SB-58M) (Baumgartner et al. 2010) and 60-Month AGN survey
145 catalog (SB-AGN) (Ajello et al. 2012), and Gamma-ray: 2nd Fermi large area telescope
146 AGN catalog (2LAC) (Ackermann et al. 2011). In each catalog, we select only those
147 objects that have redshift information. In the case of the 2LAC catalog, this criterion
148 reduces the number of objects by $\sim 50\%$.

149 The paper is organized as follows. The observation status of the SD array and qualities
150 of reconstructed events are briefly described in Section 2. The details of the parameter
151 scanning in the correlation searches using the object catalogs are given in Section 3, and
152 the results are described in Section 4. We also investigated penalties for the multi-catalog
153 scanning in Section 5. The conclusions from this analysis are in Section 6.

154 2. SD DATA

155 In this work we use the SD air shower events observed in the first 40-month run of
156 TA from May 2008 through September 2011. These events are triggered by a three-fold
157 coincidence of adjacent SDs within $8\mu\text{s}$ (Abu-Zayyad et al. 2012c).

158 The details of SD event reconstruction are described elsewhere (Ivanov et al. 2012;
159 Abu-Zayyad et al. 2012b). First, the shower geometry including the arrival direction is
160 obtained using the time differences between the observed signals at each SD. Next, the
161 precise shower geometry and the lateral distribution of shower particles are determined using
162 the observed energy deposit in each SD. Finally, the primary energy is determined from the
163 lateral distribution. The overall energy scale of the SD events is fixed by calibration with the
164 FD energy scale using a hybrid event set as described in the reference (Abu-Zayyad et al.

165 2011). The systematic uncertainty in energy determination is 22%.

166 The data quality cuts for the reconstructed events are the same as in the previous
 167 TA analysis papers (Abu-Zayyad et al. 2012a,b). The events are cut if the zenith angle
 168 is greater than 45° and/or the core position is within 1200 m of the SD array boundary.
 169 The EAS reconstruction efficiency under these criteria is greater than 98% including the
 170 duty cycle of the SD array for $E > 10$ EeV (Abu-Zayyad et al. 2012b,c). The accuracy in
 171 arrival direction determination is 1.5° and the energy resolution is better than 20% in this
 172 energy range.

173 The number of events remaining after reconstruction and quality cuts is 988 for
 174 $E \geq 10$ EeV, 57 for $E \geq 40$ EeV, and 3 for $E \geq 100$ EeV. From our Monte-Carlo studies
 175 including the full detector response simulations, we confirmed that the acceptance of the SD
 176 array is fully geometrical, i.e., independent of the arrival direction up to $\theta = 45^\circ$ for showers
 177 with energies greater than 10 EeV (Abu-Zayyad et al. 2012a,b,c). We also confirmed that
 178 the arrival direction distribution of the observed events in the horizontal coordinates and
 179 the equatorial coordinates are consistent with large scale isotropy shown in Figure 1. In
 180 this analysis, we use the geometrical acceptance to generate random events for reasons
 181 of computational efficiency. The total exposure of the SD array in the first 40 months of
 182 operation is 3.1×10^3 km² sr yr including the quality cuts.

183 3. CORRELATION ANALYSIS

184 3.1. OBJECT CATALOGS

185 We use the catalogs of extragalactic objects resulting from measurements as listed in
 186 Table 2. In several catalogs, the objects near the Galactic plane are excluded to avoid
 187 incompleteness from the experimental limitation by the authors of each catalog. We also

188 exclude the observed SD events in the corresponding regions.

189 The target objects and the cut criteria in the each catalog are summarized below.
 190 These criteria (e.g. significance level) were chosen by the authors of the each catalog.
 191 The 3CRR catalog contains radio galaxies detected at 178 MHz with fluxes greater
 192 than 10 Jy (Laing, Riley & Longair 1983). Objects in the direction of the Galactic disk
 193 ($|b| < 10^\circ$) were not included. The 2MRS (Huchra et al. 2012) catalog is derived from the
 194 2MASS observation with detection range between $1 - 2 \mu\text{m}$ and $K_s \leq 11.75$ magnitude.
 195 This catalog also loses completeness near the Galactic plane, so the authors of the catalog
 196 excluded regions with $|b| < 5^\circ$ for $30^\circ \leq l \leq 330^\circ$ and $|b| < 8^\circ$ otherwise. The SB-58M
 197 catalog consists of objects which were detected with a significance greater than 4.8σ in the
 198 energy range of 14 – 195 keV in the first 58 months of observation by Swift BAT. We select
 199 the extragalactic objects in this catalog for this work. The catalog of SB-AGN contains
 200 AGNs with at least 5σ significance in the energy range of 15 – 55 keV in the first 60 months
 201 of observation by Swift BAT. The 2LAC (Ackermann et al. 2011) data set consists of
 202 AGNs detected with at least 4σ significance in the energy range of 100 MeV–100 GeV in
 203 the first 24 months of observation by Fermi-LAT. The region of the Galactic disk $|b| < 10^\circ$ is
 204 cut away. We also examine the VCV catalog which is a compilation of several AGN surveys.
 205 The number of objects and the SD events after the cuts applied in each case are given in
 206 Table 3.

207 **3.2. METHODS**

208 For a given set of parameters $(E_{\min}, \psi, z_{\max})$, there are N events with energies
 209 $E \geq E_{\min}$. We can count the number of events, k , out of N which are correlated with
 210 objects in a catalog with redshifts $z \leq z_{\max}$ and within the angular separation ψ . We
 211 can calculate the chance probability, P , that k or more correlated events are found from

212 an isotropic UHECR flux under the same conditions. We carry out a parameter scan in
 213 $(E_{\min}, \psi, z_{\max})$ space to find the set of parameters which maximizes the correlation between
 214 the TA events and the catalog objects, i.e., minimizes P . To determine the probability, P ,
 215 we first obtain the probability, p , that a random event is correlated with at least one object
 216 by chance for a given (ψ, z_{\max}) . We generate 10^4 random events to obtain the probability,
 217 p , in the same experimental region of the each catalog.

218 Then P can be obtained as a cumulative binomial probability:

$$P = \sum_{j=k}^N C_j^N p^j (1-p)^{N-j}. \quad (1)$$

219 The scan over parameters was performed as follows. The value of E_{\min} is set by the
 220 energy of the N -th highest energy event. We scan over all values of N such that E_{\min} is
 221 greater than 40 EeV. Note that this energy is less than the energy (50 EeV) at which the
 222 TA energy spectrum begins to fall off steeply (Abu-Zayyad et al. 2012b). We set the upper
 223 boundary of the parameter z_{\max} as 0.03, which corresponds to the distances smaller than
 224 120 Mpc. This is comparable to the GZK horizon. The selected step size of z_{\max} is 0.001,
 225 which is the typical accuracy in the redshift measurements. The separation angle, ψ , is
 226 varied from 1° to 15° . The maximum search window of $\psi = 15^\circ$ is selected as appropriate
 227 for lower energy events (~ 40 EeV) arriving from the distance of 100 Mpc. The selected step
 228 size in ψ is chosen as 0.1° for $\psi < 8^\circ$ and 1° for $8^\circ \leq \psi \leq 15^\circ$. The parameter ranges and
 229 step sizes are summarized in Table 1.

230 The minimum P obtained from this procedure does not represent the correlation
 231 probability directly, because the parameter scanning enhances the correlation probability
 232 artificially (Tinyakov & Tkachev 2004). Therefore, a penalty for parameter scanning
 233 should be evaluated and the true probability of correlation must include this penalty. This
 234 will be described in Section 4.

4. RESULTS

4.1. RESULTS OF THE PARAMETER SCAN ANALYSIS

The results of the parameter scan are listed in Table 4. The smallest value of P_{\min}^{obs} among all the catalogs is 1.3×10^{-5} found in the SB-AGN catalog with the best parameters $(E_{\min}, \psi, z_{\max})_{\text{best}} = (62.20 \text{ EeV}, 10^\circ, 0.020)$. A sky map of the TA events and the objects under the condition $(E_{\min}, \psi, z_{\max})_{\text{best}}$ which gives the smallest P_{\min}^{obs} is shown in Figure 2. All the observed UHECRs with $E \geq E_{\min}$ correlate with at least one object with $z \leq z_{\max}$ in the SB-AGN catalog. Figure 3, and 4 show the probability as a function of each parameter $(E_{\min}, \psi, z_{\max})_{\text{best}}$ while fixing the values of the other two at the optimum value for this data comparison.

Now let us consider the penalty for the parameter scanning. We evaluate the probability, P_{PPS} , of finding a correlation by chance with P_{\min}^{sim} smaller than that obtained from the data as follows (for a more detailed description of the penalty calculation see, e.g., Tinyakov & Tkachev 2004). We generate 10^4 random sets of N “cosmic ray events”, where N is the same as the number of the observed events with energies greater than 40 EeV. For each of the mock event sets, the parameter scanning was carried out using exactly same method as for the observed data set, and P_{\min}^{sim} was calculated. Note that the parameters $(E_{\min}, \psi, z_{\max})_{\text{best}}$ which yield P_{\min}^{sim} are different for each of the 10^4 trials. The distribution of P_{\min}^{sim} in case of the SB-AGN catalog is shown in Figure 5 together with P_{\min}^{obs} . One can see that rather small values $P_{\min} \leq 1.3 \times 10^{-5}$ can happen even though the simulated UHECR distribution is isotropic.

If we repeat the same experiment and the parameter scanning many times, the value of our result $P_{\min}^{\text{obs}} = 1.3 \times 10^{-5}$ could be just a chance occurrence. The probability including the Penalty for the Parameter Scanning (PPS) is evaluated as $P_{\text{PPS}} = 0.01$ for the SB-AGN

259 catalog, and the values for all the catalogs are listed in Table 4. The smallest value of P_{PPS}
 260 among the catalogs is 0.01 from the the SB-AGN catalog. This does not yet include the
 261 penalty for searching in several catalogs.

262 If we have several catalogs, regardless of whether they are independent or partially
 263 overlapping, there is a possibility of finding a catalog which gives the same or smaller
 264 $P_{\text{min}}^{\text{obs}}$ value by chance, even though there are no correlations between the events and the
 265 objects. The straightforward way to calculate the penalty factor associated with the
 266 partially overlapping catalogs, as is the case in our analysis, is to include all the catalogs
 267 in the Monte-Carlo simulation. Therefore, we have repeated the simulation with 10^4 mock
 268 sets as described above, but with the scanning performed in all six catalogs. Calculating
 269 the fraction of mock sets that show equal or better correlation than the data, we find
 270 that the final probability with a Penalty of Parameter Scanning (PPS) and a Penalty of
 271 multi-Catalog Scanning (PCS) $P_{\text{PPS+PCS}} = 0.09$. Therefore, we conclude that no significant
 272 correlation between UHECRs and the astronomical objects is found in the current TA data
 273 set.

274 4.2. UNCERTAINTIES

275 First, we consider the effect of finite resolution in the scanning parameters. The
 276 uncertainty in determination of the arrival directions and energy only make correlations
 277 worse due to direction smearing and the contamination of the lower energy events than
 278 E_{min} . Therefore, the obtained $P_{\text{min}}^{\text{obs}}$ already includes these resolution effects. The same
 279 concerns the uncertainty in the redshifts of the catalog objects.

280 Consider now the effect of the systematic uncertainty in energy determination. As
 281 mentioned above, this uncertainty is 22% (Abu-Zayyad et al. 2011). Note, however, that

282 the present analysis with the parameter scanning is independent of absolute energy scale:
 283 the *energies* of the events are no more than keys for event sorting, and a systematic energy
 284 shift does not affect the scanning in E_{\min} , hence the number of events involved in the
 285 correlation with the objects and the probability P_{\min}^{obs} .

286 The last issue to discuss is the incompleteness of the catalogs, which remains even
 287 after we cut out the regions around the Galactic plane. The objects in the VCV catalog
 288 are inhomogeneous because it is a mere compilation of objects detected under different
 289 conditions. The completeness of the other catalogs, in particular the 2LAC, could be
 290 affected by our cuts, particularly by the selection of objects with the known redshift. While
 291 the incompleteness may make the *interpretation* of correlations ambiguous if they are
 292 present, it does not affect the calculation of P_{\min}^{obs} . In fact, the effect of the incompleteness
 293 cancels out in P_{\min}^{obs} since the same set of objects is used to cross-correlate with the data and
 294 each mock event set. Therefore, the incompleteness of the catalogs cannot produce spurious
 295 correlations (although it may, in principle, be responsible for their absence).

296 5. DISCUSSION

297 5.1. SEARCH FOR CORRELATIONS WITH A SPECIFIC TYPE OF 298 OBJECT

299 So far we have treated the objects in each catalog equally regardless of their class.
 300 Now let us examine whether there is a specific type of object that has stronger correlations
 301 with UHECRs than others. We will consider the case of the SB-AGN catalog which shows
 302 strongest correlations with UHECRs.

303 First, we count the number of objects of each class in the TA FOV with redshifts
 304 smaller than 0.02. Some of the objects are labeled “unclassified” in the catalog. For

305 these we used the information from other surveys (Noguchi et al. 2010; Parisi 2011;
 306 Veron-Cetty & Veron 2010; Baumgartner et al. 2010). The fractions of Seyfert 2, 1, 1.5,
 307 1.9 and LINER galaxies in the SB-AGN catalog satisfying the above conditions are 0.441,
 308 0.235, 0.132, 0.044, and 0.044, respectively (the total fraction of other class AGNs: 0.044,
 309 and the fraction of the unclassified AGN: 0.059). The total number of AGNs which are
 310 correlated with UHECRs is 22 with the parameters in Table 4 (note that the number of
 311 UHECR events and that of AGNs are not the same because some of the events fall within
 312 the given angular distance from several sources). Among these 22 AGNs the fractions of
 313 Seyfert 2, 1, 1.5, 1.9, LINER, and unclassified galaxies are 0.455, 0.182, 0.227, 0.045, 0.045,
 314 and 0.045, respectively. We see that the largest difference is for the Seyfert 1.5 galaxies.
 315 The probability, P , of finding 5 or more correlated Seyfert 1.5 galaxies out of 22 by chance
 316 can be evaluated by the cumulative binomial probability with an expectation of 0.13, and is
 317 $P = 0.16$. Therefore, no significant correlation with a specific type of AGN in the SB-AGN
 318 catalog is found.

319 6. CONCLUSION

320

321 We examine the correlations between the observed UHECR arrival directions and the
 322 extragalactic objects from the different survey catalogs under assumption that the sources
 323 have the same intrinsic UHECR luminosities. We use the TA-SD events with energies
 324 greater than 40 EeV obtained in the first 40 months of observation. We search for maximum
 325 correlations by scanning over three parameters E_{\min} , ψ , and z_{\max} in six different catalogs.
 326 The smallest chance probability among these six catalogs was found with the Swift BAT
 327 (60-month) AGN catalog, $P_{\min}^{\text{obs}} = 1.3 \times 10^{-5}$. This probability increases to $P_{\text{PPS}} = 0.01$
 328 when we include the penalty for the three-parameter scanning in the Swift BAT catalog

329 alone, and to $P_{\text{PPS+PCS}} = 0.09$ when scanning in all the catalogs is taken into account.
330 Therefore, we conclude that no significant correlation with the considered catalogs of
331 extragalactic objects is found in the present TA data set. Investigating specifically the case
332 of the Swift BAT (60-month) AGN catalog which gives the strongest correlation, we find
333 that no particular subclass of objects is responsible for this correlation.

334 The Telescope Array experiment is supported by the Japan Society for the Promotion
335 of Science through Grants-in-Aid for Scientific Research on Specially Promoted Research
336 (21000002) “Extreme Phenomena in the Universe Explored by Highest Energy Cosmic
337 Rays”, and the Inter-University Research Program of the Institute for Cosmic Ray
338 Research; by the U.S. National Science Foundation awards PHY-0307098, PHY-0601915,
339 PHY-0703893, PHY-0758342, PHY-0848320, PHY-1069280, and PHY-1069286 (Utah) and
340 PHY-0649681 (Rutgers); by the National Research Foundation of Korea (2006-0050031,
341 2007-0056005, 2007-0093860, 2010-0011378, 2010-0028071, R32-10130); by the Russian
342 Academy of Sciences, RFBR grants 10-02-01406a and 11-02-01528a (INR), IISN project
343 No. 4.4509.10 and Belgian Science Policy under IUAP VI/11 (ULB). The foundations of
344 Dr. Ezekiel R. and Edna Wattis Dumke, Willard L. Eccles and the George S. and Dolores
345 Dore Eccles all helped with generous donations. The State of Utah supported the project
346 through its Economic Development Board, and the University of Utah through the Office
347 of the Vice President for Research. The experimental site became available through the
348 cooperation of the Utah School and Institutional Trust Lands Administration (SITLA),
349 U.S. Bureau of Land Management and the U.S. Air Force. We also wish to thank the
350 people and the officials of Millard County, Utah, for their steadfast and warm support. We
351 gratefully acknowledge the contributions from the technical staffs of our home institutions
352 as well as the University of Utah Center for High Performance Computing (CHPC).

REFERENCES

353

354 Abbasi R.U., et al. 2008, *Astropart. Phys.*, 30, 175

355 Abbasi, R.U., et al. 2008, *Phys.Rev.Lett.*, 100, 101101

356 Abraham, J., et al., 2008, *Phys.Rev.Lett.*, 101, 061101

357 Abraham, J., et al. 2010 *Phys.Lett.B*, 685, 239

358 Abu-Zayyad T., et al., 2011 Proceedings of 32nd International Cosmic Ray Conference, 2,

359 250

360 Abu-Zayyad T., et al., 2012a, *ApJ*, 757, 26

361 Abu-Zayyad T., et al., 2012b, arXiv:1205.5067.v1

362 Abu-Zayyad T., et al. 2012c, *Nucl. Instr. and Meth. A*, 689, 87

363 Abreu P., et al. 2007, *Science*, 318, 938

364 Abreu P., et al. 2008, *Astropart. Phys.*, 29, 188

365 Abreu P., et al. 2010, *Astropart. Phys.*, 34 314

366 Ackermann M., et al. 2011, *ApJ*, 743, 171

367 Ajello M., et al. 2012, *ApJ*, 749, 21

368 Tueller J., Baumgartner W.H., Markwardt C.B., et al. 2010, *ApJS*, 186, 378 the latest data

369 taken from <http://heasarc.nasa.gov/docs/swift/results/bs58mon/>

370 Greisen, K. 1966, *Phys.Rev.Lett.*, 16, 748

371 Han, J.L., Manchester, R.N., Lyne, A.G., Qiao,G.J., & van Straten, W. 2006, *ApJ*, 642, 868

- 372 Huchra, J.P., et al. 2012 ApJS, 199, 26
- 373 Ivanov, D., et al. 2011, Proceedings of 32nd International Cosmic Ray Conference, 2, 258
- 374 Kawai, H., et al. 2008, Nucl. Phys. B Proc. Suppl, 175-176, 221
- 375 Kotera K. & Olinto A.V. 2011, Annu. Rev. Astron. Astr. 49, 119
- 376 Kronberg, P.P. 1994, Rept. Prog. Phys., 57, 325
- 377 Laing, R.A., Riley, J.M., & Longair, M.S. 1983, MNRAS, 204, 151, data taken from
378 <http://3crr.extragalactic.info>
- 379 Matthews, J.N., et al. 2007 Proceedings of 30th International Cosmic Ray Conference, 5,
380 1157
- 381 Noguchi, K. et al, arXiv:1002.0909
- 382 Parisi, P., arXiv:1105.0527
- 383 Pshirkov, M., Tinyakov, P., Kronberg, P., & Newton-McGee, K. 2011, Astrophys.J., 738,
384 192
- 385 Sun, X.H., Reich, W., Waelkens, A., Enßlin, T.A. 2008, A&A, 477, 573
- 386 Takeda, M., et al. 1998, Phys. Rev. Lett., 81, 1163
- 387 Takeda, M., et al. 2003, Astropart. Phys., 19, 447
- 388 Tokuno H., et al. 2012, Nucl. Instr. and Meth. A, 676, 54
- 389 Tinyakov, P.G., & Tkachev, I. I. 2004, PRD, 69, 128301
- 390 Veron-Cetty, M.P., & Veron, P. 2006 Astrophys., 455, 773
- 391 Veron-Cetty, M.P., & Veron, P. 2010 A&A, 518, A10

³⁹² Zats'epin, G.T., & Kuz'min, V.A. 1966, JET PLet., 4, 78

Parameter	Range	Step size
Energy (EeV)	$E \geq 40$	Energy of each event by sorted order
Redshift (z)	$0.001 \leq z \leq 0.030$	0.001
Window (degree)	$1 \leq \psi < 8$	0.1
	$8 \leq \psi \leq 15$	1

Table 1: List of the scan regions and step size for each scan parameter.

Catalog	Range	N_{all}	N_{target}
3CRR	compilation of Radio surveys	173	16
2MRS	IR ($1-2\mu\text{m}$)	43533	13547
SB-58M	X-ray ($14 - 195 \text{ keV}$)	1092	161
SB-AGN	X-ray ($15 - 55 \text{ keV}$)	428	102
2LAC	γ -ray ($100 \text{ MeV} - 100 \text{ GeV}$)	1126	6
VCV	compilation of AGNs	168941	762

Table 2: List of the configuration of the used catalogs. N_{all} : number of all objects contained within the catalog, N_{target} : number of objects with the redshift $z < 0.03$ within the TA FOV.

Catalog	Cut region (degree)	N ($E \geq 40$ EeV)
3CRR	$ b < 10^\circ, \delta < 10^\circ$	41
2MRS	$ b < 5^\circ$ for $30^\circ \leq l \leq 330^\circ$	56
	$ b < 8^\circ$ otherwise	
SB-58M	None	57
SB-AGN	None	57
2LAC	$ b < 10^\circ$	49
VCV	None	57

Table 3: List of the cut region away from the Galactic plane of the each catalog and the number (N) of events remaining (the maximum number is 57). Symbols mean: b : Galactic latitude, l : Galactic longitude, δ : declination of the equatorial coordinate.

Catalog	E_{\min} (EeV)	ψ (degree)	z_{\max} (z)	A	N	k	p	P_{\min}	P_{PPS}
3CRR	66.77	2.0	0.017	4	11	1	0.0020	2.2×10^{-2}	0.75
2MRS	51.85	6.5	0.005	660	31	29	0.62	8.5×10^{-5}	0.21
SB-58M	57.46	11	0.017	79	25	25	0.68	6.1×10^{-5}	0.04
SB-AGN	62.20	10	0.020	58	17	17	0.52	1.3×10^{-5}	0.01
2LAC	55.41	12	0.018	3	23	3	0.069	2.1×10^{-1}	0.83
VCV	62.20	2.1	0.016	288	17	8	0.14	8.6×10^{-4}	0.25

Table 4: Summary of correlations with the best parameter set (minimum threshold, Window size, maximum redshift) for each catalog. A : number of objects with the redshift $\leq z_{\max}$, N : number of observed cosmic ray events with the energy $E \geq E_{\min}$, k : number of events correlated with objects, p : probability of correlation for a single event from an isotropic distribution, P_{\min} : the cumulative binomial probability to obtain k or more estimated from an isotropic distribution, P_{PPS} : the probability after including the penalties from parameter scanning.

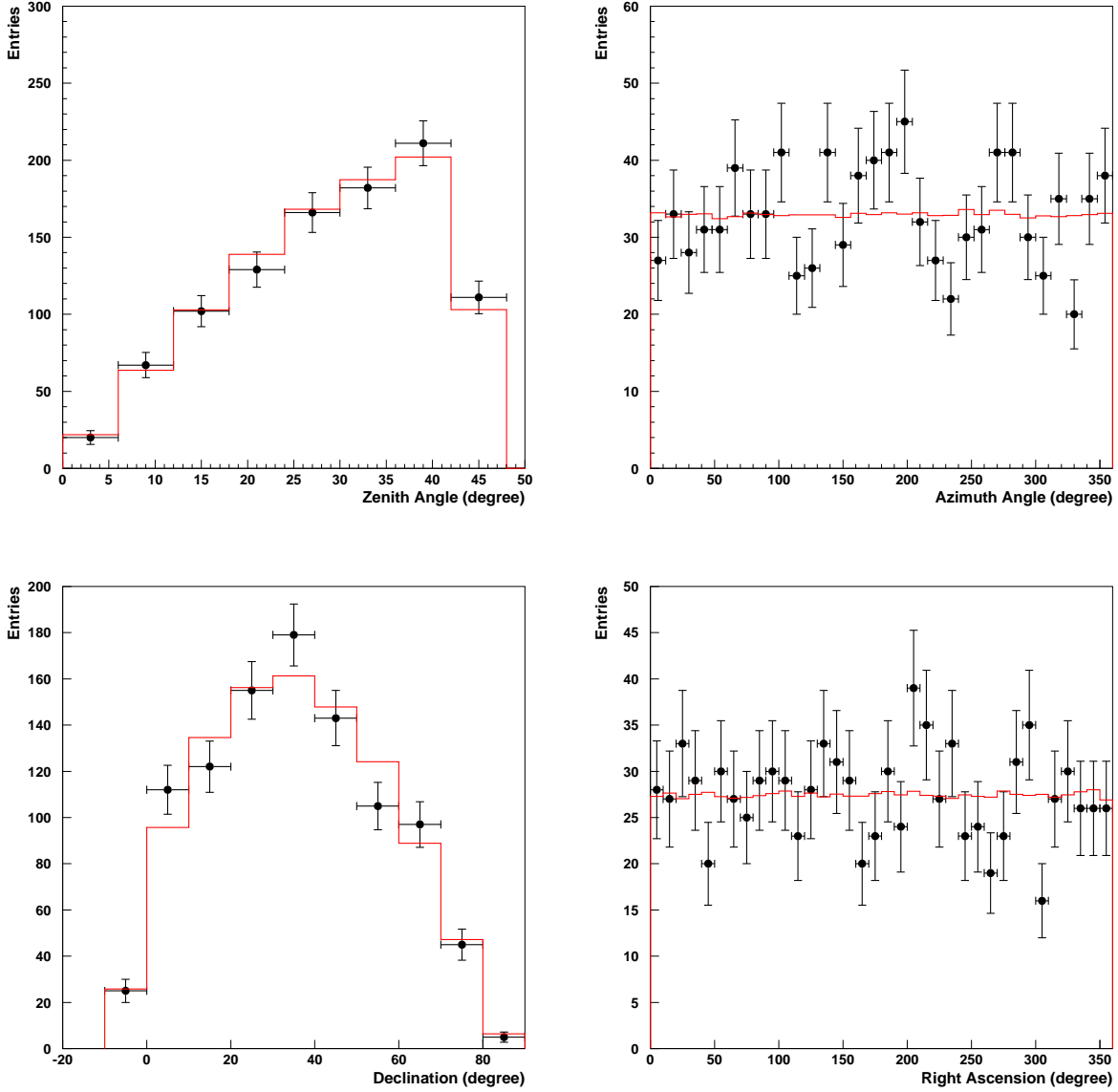


Fig. 1.— The distribution of observed data (plot) and the simulated data with the geometrical acceptance (histogram) with the energy > 10 EeV. The top left: zenith angle, the top right: azimuth angle, the bottom left: declination, and the bottom right: right ascension.

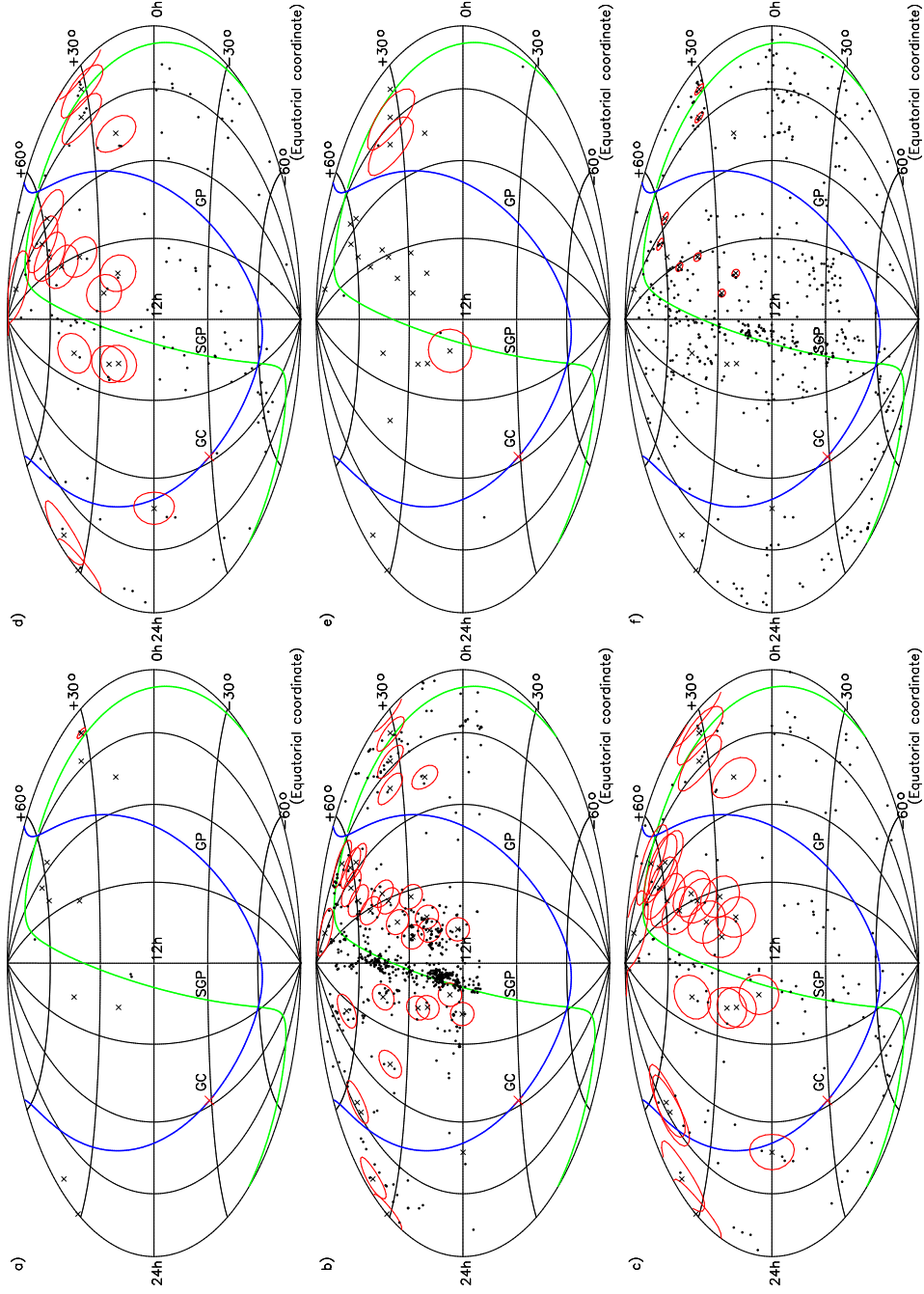


Fig. 2.— Arrival directions of observed UHECR with the objects of the each catalog (a: 3CRR, b: 2MRS, c: SB-58M, d: SB-AGN, e: 2LAC, and f: VCV). Dots: catalog objects, x: arrival direction of observed cosmic rays, Circle: window around cosmic ray events, GC: Galactic Center, GP: Galactic Plane, SGP: Super Galactic Plane.

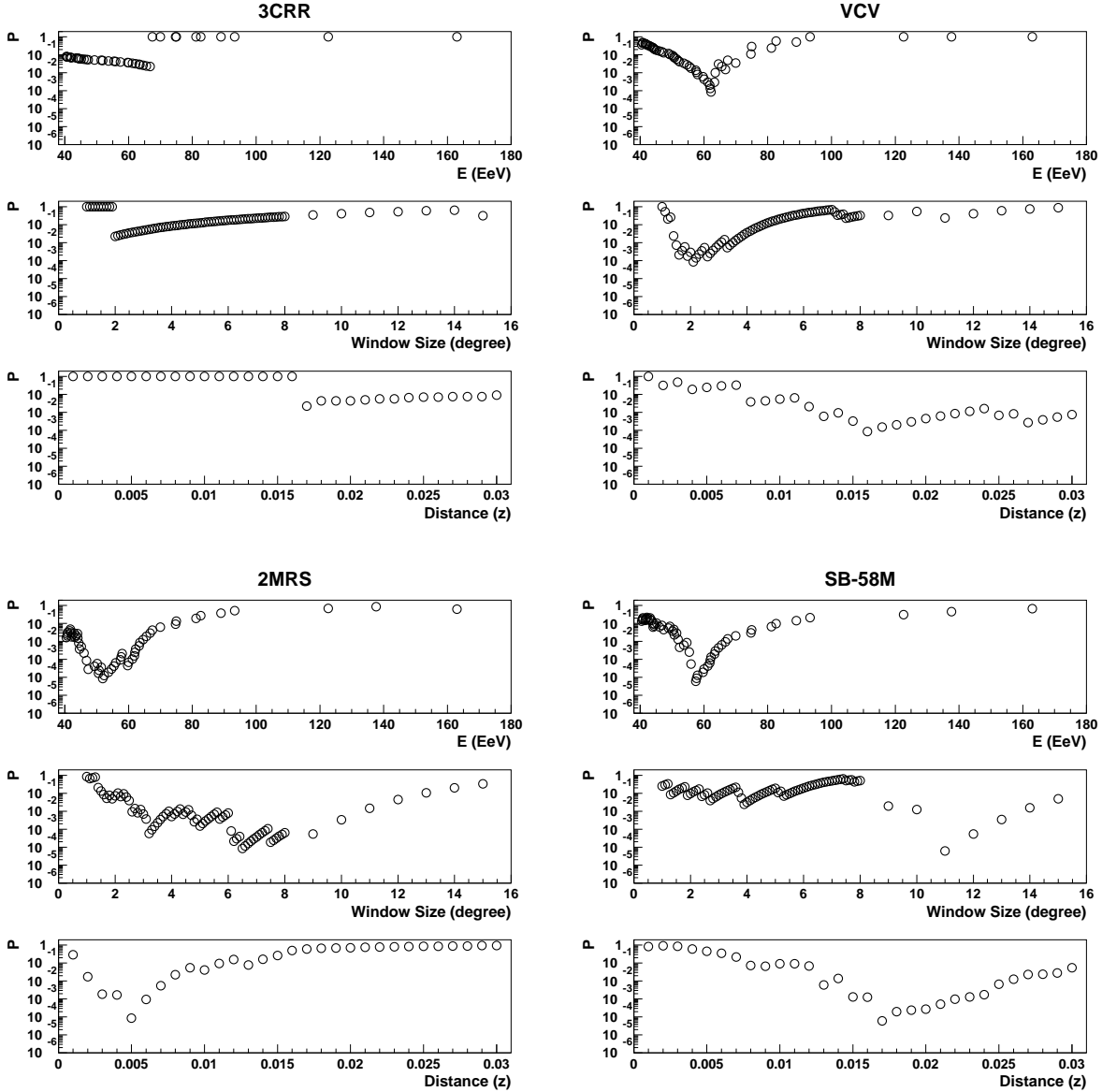


Fig. 3.— Cumulative binomial probability distribution for the 3CRR (top left panel), VCV catalog (top right panel), 2MRS (bottom left panel), and SB-58M (bottom right panel). Each panel shows the probability distribution with Energy threshold (E_{\min}) of observed cosmic rays (top), window ψ (middle), redshift z_{\max} (bottom). In the each plot, the other two parameters are fixed at which parameter set provides P_{\min} .

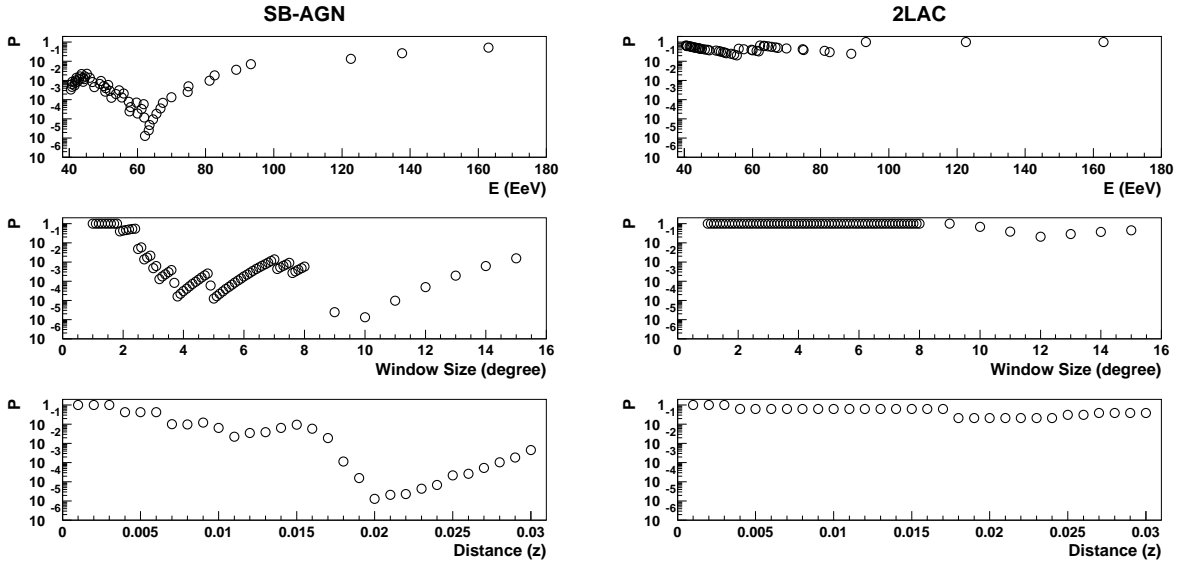


Fig. 4.— Cumulative binomial probability distribution for the SB-AGN (left panel), 2LAC (right panel). Each panel shows the probability distribution with Energy threshold (E_{\min}) of observed cosmic rays (top), window ψ (middle), redshift z_{\max} (bottom). In the each plot, the other two parameters are fixed at the optimum value.

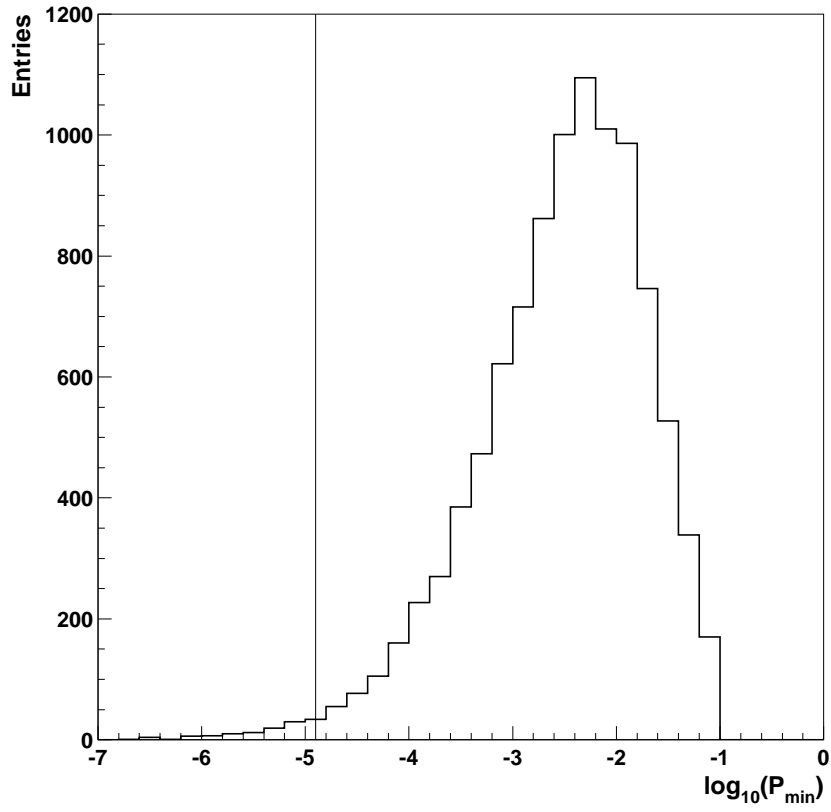


Fig. 5.— Distribution of probability P_{\min}^{sim} for SB-AGN catalog determined from 10^4 simulated isotropic data sets. The observed $P_{\min}^{\text{obs}} = 1.3 \times 10^{-5}$ is shown as a vertical line.